Biomolecules & Therapeutics, **16**, 190-196(2008)

Characterization of Deoxypodophyllotoxin Metabolism in Rat Liver Microsomes

Sang Kyu Lee, In Hye Jun, Mi Jeong Kang, Tae Won Jeon, Ju Hyun Kim, Young Min Seo, Sil Shin, Jae Ho Choi, Hye Gwang Jeong[1], Seung Ho Lee and Tae Cheon Jeong*

College of Pharmacy, Yeungnam University, Gyeongsan, 712-749, Korea
[1]College of Pharmacy, Chosun University, Gwangju, 501-759, Korea

(Received July 21, 2008; Revised August 26, 2008; Accepted August 27, 2008)

Abstract – Deoxypodophyllotoxin (DPT) is a medicinal herb product isolated from *Anthriscus sylvestris*. DPT possesses beneficial activities in regulating immediate-type allergic reaction and anti-inflammatory activity through the dual inhibition of cyclooxygenase-2 and 5-lipoxygenase. In the present study, the metabolism of DPT was further characterized in rat liver microsomes isolated from male Sprague Dawley rats. The metabolism of DPT was NADPH-dependent. In addition, when liver microsomes were incubated with SKF-525A, a well-known CYP inhibitor, in the presence of β-NADPH, the metabolism of DPT was significantly inhibited. Using enriched rat liver microsomes, the anticipated isoforms of cytochrome P450s (CYPs) in the metabolism of DPT were partially characterized. Phenobarbital-induced microsomes increased in the formation of metabolite M1. The metabolite M3 was only produced in the enriched microsomes isolated from dexamethasone-treated rats. The results indicated that the metabolism of DPT would be CYP-dependent and that CYP2B and CYP3A might be important in the metabolism of DPT in rats.

Key words: Deoxypodophyllotoxin, Metabolism, Cytochrome P450, *in vitro*, Electrospray ionization tandem mass spectrometry, Microsome

INTRODUCTION

Anthriscus sylvestris Hoffm. (*A. Sylvestris*) growing in Eurasia and eastern part of North America is a member of the *Umbelliferae* family and accumulates deoxypodophyllotoxin (DPT, Fig. 1) and other lignans in the roots.

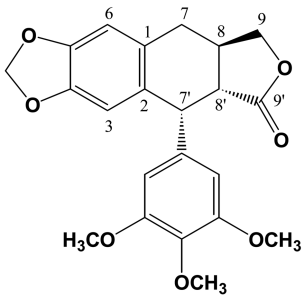

Fig. 1. Structure of DPT. Molecular weight, 398.41.

*Corresponding author
Tel: +82-53-810-2819, Fax: +82-53-810-4654
E-mail: taecheon@yumail.ac.kr

The dried root of *A. Sylvestris* has been used in oriental traditional medicines with antipyretic, analgesic and anti-cough activities. It has already been reported that DPT, a podophyllotoxin derivative lignan, possesses anti-proliferative (Ikeda *et al*., 1998), anti-platelet aggregation (Chen *et al*., 2000), anti-viral (Gordaliza *et a*l., 1994; Sudo *et al*., 1998), broad insecticidal (Inamori *et al*., 1985) and cytotoxic activities (Lim *et al*., 1999; Kim *et al*., 2002; Masuda *et a*l., 2002).

Recently, DPT has been characterized to have anti-inflammatory activity through the dual inhibition of cyclooxygenase-2 and 5-lipoxygenase in mouse bone marrow-derived mast cells (Lee *et al*., 2004). Most recently, it has been reported that DPT might abolish lipopolysaccharide-induced expression of nitric oxide synthase by inhibiting the transcription factor, NF-κB (Jin *et al*., 2008) In the mean time, DPT was converted into podophyllotoxin in experiments with plant cell suspension cultures (Molog *et al*., 2001; Koulman *et al*., 2003a, c). Podophyllotoxin is a lignan that can be used to treat genital warts (Gross *et al*., 2001). In addition, podophyllotoxin is a unique starting compound for the production of

anticancer drugs, e.g., etoposide (Koulman *et al*., 2003b). This provides a rationale for the use of *A. sylvestris* as an oriental traditional herb for treating inflammatory and allergic related disorders, and for the use of tumor treating. Meanwhile, the metabolism of DPT in mammalian systems has not been extensively characterized although DPT was converted to epipodophyllotoxin by cDNA-expressed human cytochrome P450 (CYP) 3A4 (Vasilev *et al*., 2006).

Recently, tandem mass spectrometric technique has widely been used for qualitative and quantitative analysis in many areas of research (Myung *et al*., 2002). Recently, we have identified 7 metabolites of DPT from the incubation of DPT with human and rat liver microsomes and assigned possible structures of these metabolites by using this technique (Lee *et al*., 2008). Therefore, the primary objective of the present study was to further characterize the *in vitro* metabolic profiles of DPT by using high-performance liquid chromatography (HPLC) and liquid chromatography-electrospray ionization mass spectrometry (LC-ESI/MS). Following an incubation of DPT with rat liver microsomes, the formation of DPT metabolites was characterized. The secondary goal was to characterize the major enzymes involved in DPT metabolism in enriched rat liver microsomes.

MATERIALS AND METHODS

Materials

DPT (purity, > 98%) used in this study was isolated from dried roots of *A. sylvestris* (Lee *et al*., 2004). Its chemical structure was established by comparison of ^{1}H- and ^{13}C-NMR and optical rotation data obtained with those reported previously (Bogucki and Charlton, 1995). Glucose 6-phosphate (G6P), β-NADPH, glucose 6-phosphate dehydrogenase (G6PDH), dexamethasone, and phenobarbital were obtained from Sigma Chemical Co. (St. Louis, MO, USA). Methanol (MeOH) was HPLC-grade from Merck Ltd. (Poole, UK). 3-Methylcholanthrene and acetic acid were obtained from Aldrich Chemical Co. (Milwaukee, WI, USA). Acetone was the first grade from Duksan Pure Chemicals Co. (Ansan, Gyungkido, Korea). All other reagents used were of analytical grade and used as received.

Animal treatment

Specific pathogen-free male Sprague-Dawley rats (270-300 g) were obtained from Orient Co. (Seoul, Korea). The animals received at 5-6 weeks of age were acclimated for at least 1 week. Upon arrival, animals were randomized and housed two per cage. The animal quarters were strictly maintained at 23 ± 3°C and 50 ± 10% relative humidity. A 12 h light and dark cycle was used with an intensity of 150-300 Lux. For CYP enrichment, rats were pretreated with either 3-methylcholanthrene (40 mg/kg, i.p., 3 days) in corn oil, dexamethasone (50 mg/kg, i.p., 3 days) in corn oil, phenobarbital (80 mg/kg, i.p., 3 days) in saline, or acetone (5 ml/kg, p.o., once). Twenty-four hr after the last dose in case of 3-methylcholanthrene, dexamethasone and phenobarbital, and two days after the last dose in case of acetone, the animals were sacrificed to prepare liver microsomes.

Preparation of liver microsomes

The livers were perfused with ice-cold saline to remove excess blood and homogenized with four volumes of ice-cold 0.1 M potassium phosphate buffer, pH 7.4. The liver homogenates were centrifuged at 9,000×g for 10 min at 4°C and the resulting post-mitochondrial supernatants were centrifuged again at 105,000×g for 60 min at 4°C. The microsomal pellets were resuspended in 0.1 M potassium phosphate buffer, pH 7.4, containing 20% glycerol (Lee *et al*., 2008). Aliquots of liver microsomes were stored at -80°C until use. The content of microsomal protein was determined according to the method of Lowry *et al*. (1951), using bovine serum albumin as a standard.

Biotransformation of DPT

Metabolism of DPT (50 μM, final concentration) was determined with 1 mg/ml of microsomal protein in 0.1 M potassium phosphate buffer, pH 7.4, at 37°C for 60 min in a final incubation volume of 500 μl. The reactions were initiated by the addition of an NADPH-generating system containing 0.8 mM β-NADPH, 10 mM G6P and 1 unit of G6PDH into the reaction mixture. The reaction was stopped after incubation by the addition of 750 μl ethyl acetate. After mixing and centrifugation, 500 μl of the organic layer was separated. The extraction step was repeated three times. The organic layer was dried under a stream of nitrogen gas. A residue was reconstituted in an HPLC grade MeOH and injected into an HPLC column and an LC-ESI/MS column.

LC-ESI/MS

The HPLC consisted of a surveyor system with the LCQ advantage trap mass spectrometer (Thermo Finnigan, San Jose, CA, USA) equipped with an ESI source. The column used for the separation was an XTerra® MS C_{18} 3.5 μm (2.1 × 100 mm). The HPLC mobile phases consisted of aqueous 0.2% acetic acid (A) and 100%

MeOH (B) (Wong *et al*., 2000). A gradient program was used for the HPLC separation at a flow rate of 160 μl/min. The initial composition was programmed 30% B, and the final was programmed linearly to 70% B during 32 min. Initial stage program for 5 min was needed to stabilize MS for the next sample. In the ESI source parameters, nitrogen was used both as the sheath gas at a flow rate of 400 μl/min and as the auxiliary/sweep gas at a flow rate of > 10 μl/min. ESI spray voltage was set at 5.30 kV. Capillary temperature was set at 275°C and capillary voltage was set at 1.50 V. Tube lens offset was at 58.80 V. The mass spectrometer was operated in the positive-ion mode in *m/z* range of 50-500. Helium was used as the collision gas for the tandem mass spectrometric experiments, followed by the isolation of individual ions over a selected mass window of 1 Da.

HPLC

HPLC analyses of DPT and its metabolites in microsome-incubated samples were performed with a PU610 pump and a UV620 detector (GL Sciences Inc., Tokyo, Japan). The samples (20 μl) were injected into the chromatographic system and separated on an Intertsil® ODS-3 column, 5 μm (4.6 × 150 mm, GL Sciences Inc., Tokyo, Japan) with a Phenomenex® SecurityGuard™ guard cartridge C18 (4 mm, 3.0 mm I.D., Torrance, CA, USA). Separation was conducted with a linear gradient system from 30 : 70 to 70 : 30 during 17 min (100% MeOH : 0.2% acetic acid) and then maintained 30 : 70 mobile phase during 6 min. The analyses were performed at 40°C with a flow rate of 1.0 ml/min and UV detection at 285 nm.

Statistics

The mean value ± standard error (S.E.) was determined for each treatment group of a given experiment. Student t-test was used to compare statistical significance of data. The significant values at either $P < 0.05$ (*) or $P < 0.01$ (**) were represented as asterisks.

RESULTS

Role of CYP enzymes in DPT metabolism in rat liver microsomes

To identify the formation of Phase I metabolites, DPT was incubated with rat liver microsomes in the presence of NADPH-generating system for 60 min. DPT was metabolized to three metabolites by uninduced rat liver microsomes and four metabolites by dexamethasone-induced rat liver microsomes in the presence of NADPH-generating system in the present HPLC condition (Figs. 2 and 3). No metabolites were generated in the absence of NADPH (Figure 2). The UV spectra of DPT and its metabolites are shown in Fig. 4. The UV spectra of DPT and its major metabolites were very similar. Subsequently, dexamethasone-induced microsomes were used for the chemical inhibition study, because the four metabolites were only detected in these microsomes. It was found that the formation of individual metabolites was significantly inhibited when 200 μM SKF-525A was added into the reaction mixture (Table I). The metabolite M1 was not produced in the presence of SKF-525A in uninduced and dexamethasone-induced rat liver microsomes. The metabolite M4 was decreased to 37.1% and 44.9% of controls by SKF-525A in uninduced and dexamethasone-induced rat liver microsomes, respectively. Taken together, the present results clearly indicated that the metabolism of DPT might be catalyzed by CYP enzymes in rat liver microsomes.

Formation of the Phase I metabolites of DPT in rat liver microsomes

From the extracted ion chromatograms, the peaks of

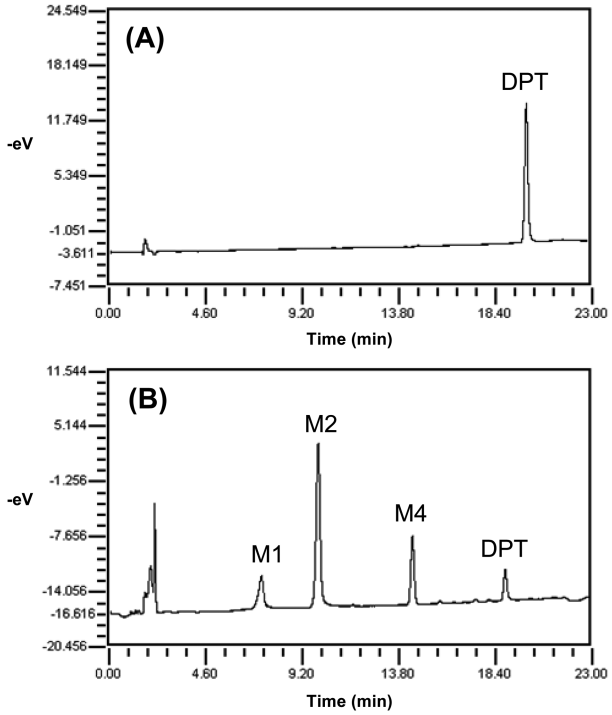

Fig. 2. LC/UV chromatograms of DPT and its metabolites in uninduced rat liver microsomes. DPT at 50 μM was incubated with uninduced rat liver microsomes (1 mg/ml) in the absence (A) or presence (B) of NADPH-generating system for 1 h at 37°C as described in the Materials and Methods.

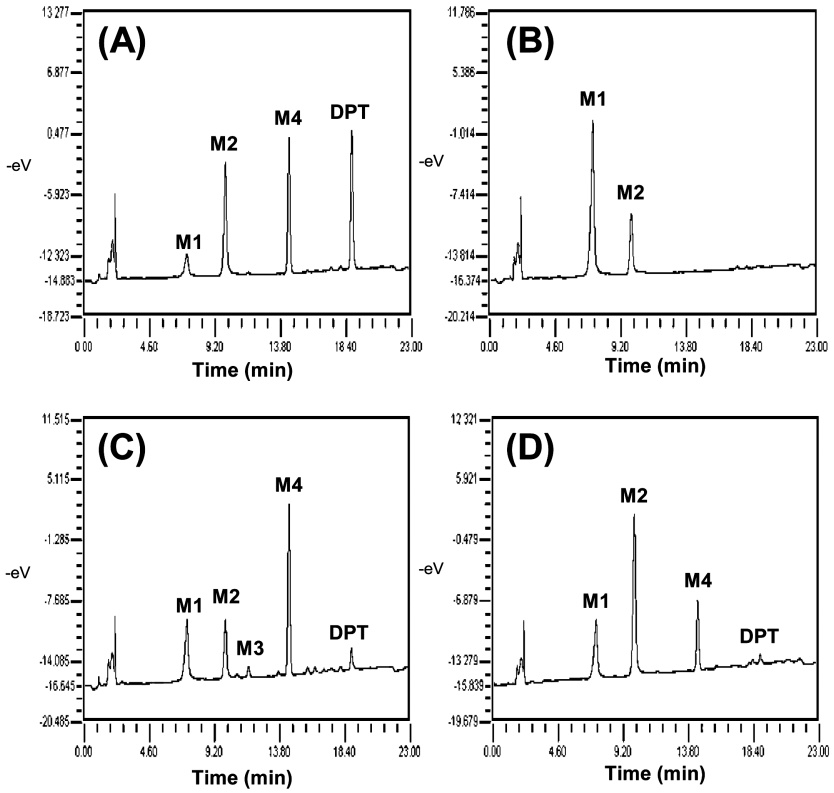

Fig. 3. LC/UV chromatograms of DPT and its metabolites in enriched rat liver microsomes. DPT at 50 μM was incubated with 3-methylcholanthrene (A), phenobarbital (B), dexamethasone (C) or acetone (D) enriched rat liver microsomes (1 mg/ml) in the presence of NADPH-generating system for 1 h at 37°C as described in the Materials and Methods.

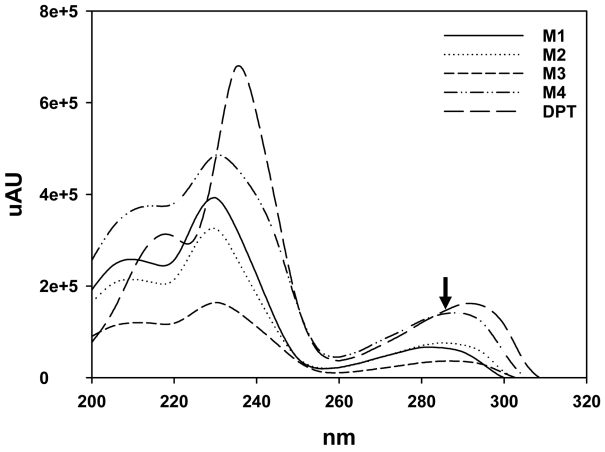

Fig. 4. UV spectra of DPT and its metabolites. An arrow indicates the wavelength at 285 nm.

DPT, M1, M2, M3 and M4 were detected at *m/z* 399, 403, 387, 401, and 415, respectively (Fig. 5). The protonated molecular ions of metabolites were identified by the full-scan MS detection. The proposed structures of individual metabolites were given in our recent report (Lee *et al*., 2008). According to the results, M4 is a mono-hydroxylated form of DPT on the C-7 position. However, the exact configuration of the hydroxyl group could not be assigned due to the limitation of MS. The results also indicated that M1 and M2 are the same as we reported, and that M3 and M4 are M4 and M7 that we reported recently (Lee *et al*., 2008).

Characterization of DPT metabolism in rat liver microsomes

To investigate the effects of different CYP isoforms on DPT metabolism, the formation of major 4 metabolites (i.e., M1, M2, M3 and M4) was determined in the incubation of DPT with uninduced, 3-methylcholanthrene-, phenobarbital-, dexamethasone- or acetone-induced rat liver microsomes (Fig. 3 and Table II). The production of metabolite M1 was increased in phenobarbital-, dexamethasone- and acetone-induced microsomes by 5.42-, 1.47- and 1.42-fold, respectively. In 3-methylcholanthrene-induced microsomes, metabolite M1 was decreased by 0.52-fold, when compared with the uninduced control microsomes. 3-Methylcholanthrene-, phenobarbital-, dex-

Table I. Effects of SKF-525A on DPT metabolism

Metabolites	Uninduced microsomes		Dexamethasone-induced microsomes	
	Without SKF-525A	With SKF-525A	Without SKF-525A	With SKF-525A
M1	100 ± 1.2	N.D.**	100 ± 7.1	N.D.**
M2	100 ± 1.5	83.0 ± 0.2**	100 ± 1.7	84.8 ± 11.1
M3	N.D.	N.D.	100 ± 4.1	N.D.**
M4	100 ± 1.2	37.1 ± 0.2**	100 ± 0.5	44.9 ± 1.2**

DPT at 50 μM was incubated with either uninduced or dexamethasone-induced rat liver microsomes (1 mg/ml) in the presence of NADPH-generating system for 1 h at 37°C either with or without SKF-525A at 200 μM. Each value represents the mean relative percent to without SKF-525A controls±S.E. of four determinations. The asterisks indicate significant differences from without SKF-525A at $P < 0.01$ (**). N.D, not detected.

Table II. Formation of DPT metabolites in uninduced and enriched rat liver microsomes

Microsomes induced by	Metabolites			
	M1	M2	M3	M4
Uninduced	100 ± 1.7	100 ± 1.6	N.D.	100 ± 2.2
3-MC	52.4 ± 2.2**	59.7 ± 1.3**	N.D.	170.6 ± 2.2**
PB	542.8 ± 6.2**	30.8 ± 1.6**	N.D.	N.D.
DEX	147.1 ± 4.7**	33.3 ± 0.8**	173590 ± 17642[a]	245.5 ± 2.8**
ACE	142.2 ± 4.3**	95.5 ± 0.6*	N.D.	100.9 ± 2.0**

DPT at 50 μM was incubated with either uninduced or enriched rat liver microsomes (1 mg/ml) in the presence of NADPH-generating system for 1 h at 37°C. Each value represents the mean relative percent to uninduced microsomes used ± S.E. of four determinations. The asterisks indicate significant differences from uninduced controls at either $P < 0.05$ (*) or $P < 0.01$ (**). [a]Value is mean area under the curve in the chromatogram ± S.E. of four determinations. N.D., not detected. 3-MC, 3-methylcholanthrene; PB, phenobarbital; DEX, dexamethasone; ACE, acetone.

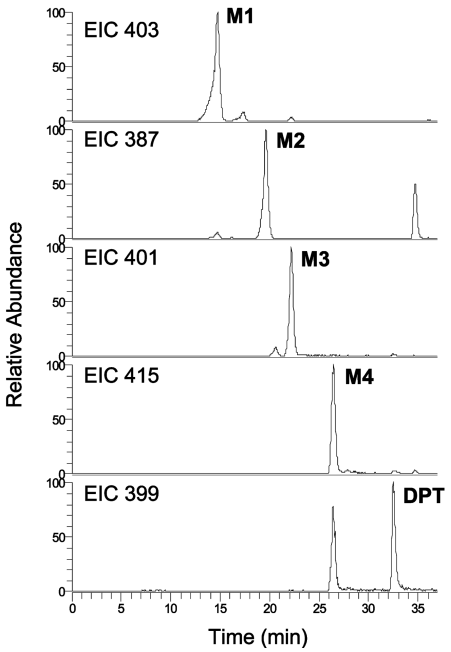

Fig. 5. Extract ion chromatograms of DPT, M1, M2, M3 and M4. DPT at 50 μM and dexamethasone enriched rat liver microsomes (1 mg/ml) were incubated in the presence of NADPH-generating system for 1 h at 37°C as described in the Materials and Methods.

amethasone- and acetone-induced microsomes allowed the formation of metabolite M2 to decrease by 0.60-, 0.31-, 0.33- and 0.96-fold, respectively. Metabolite M3 was only produced in dexamethasone-induced microsomes. The production of M4 was increased in 3-methylcholanthrene- and dexamethasone-induced microsomes by 1.7- and 2.45-fold, respectively. In phenobarbital-induced microsomes, M4 was not produced. The results clearly indicated that dexamethasone-induced liver microsomes might be able to enhance DPT metabolism predominantly, which was consistent with our recent results (Lee *et al*., 2008).

Subsequently, the formation of individual metabolites was characterized in rat liver microsomes. The formation of M2 was increased and the formation of M4 was constant when the duration of incubation time was increased in uninduced and dexamethasone-induced rat liver microsomes (Fig. 6). Metabolites M1 and M3 could be detected after M2 and M4 had been formed.

DISCUSSION

Metabolism of DPT has been reported in plant cells. In

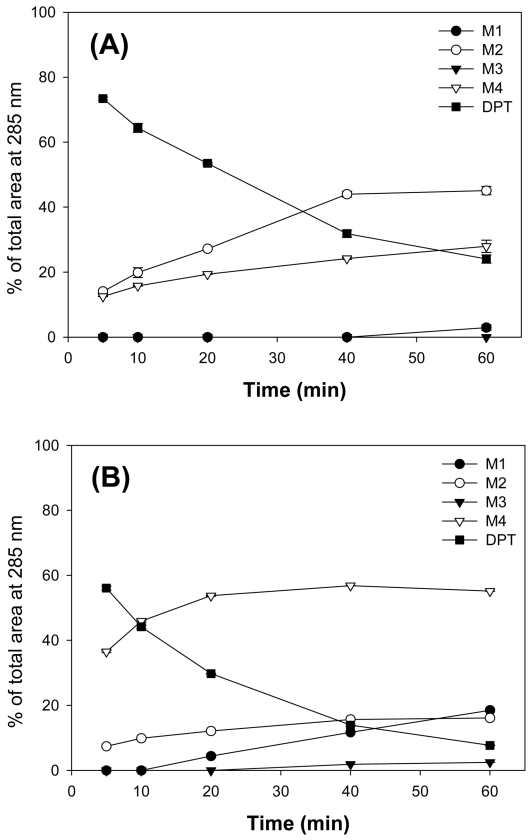

Fig. 6. Peak area-time profile of DPT and its metabolites in uninduced rat liver microsomes (A) and dexamethasone-induced rat liver microsomes (B). Incubations contained DPT at 50 μM, rat liver microsome (1 mg/ml) and an NADPH-generating system. Each point represents the mean ± S.E. of three determinations.

a cell culture of *Linum flavum*, DPT was converted to 6-methoxypodophyllotoxin via podophyllotoxin and β-peltatin, possibly by CYP-dependent reaction (Molog *et al*., 2001). In addition, the cell culture of *Linum flavum* could convert DPT to 6-methoxypodophyllotoxin glucoside (Koulman *et al*., 2003a). In mammalian systems, it has been known that DPT could be metabolized to epipodophyllotoxin by human CYP3A4 (Vasilev *et al*., 2006). Most recently, we have identified 7 different metabolites from the incubation of DPT with rat or human liver microsomes by using LC-ESI/MS techniques (Lee *et al*., 2008). In the report, it was also found that CYP3A4 and CYP2C19 would be the major CYP isozymes in the metabolism of DPT in human liver microsomes. In the present studies, the metabolism of DPT was further characterized in rat liver microsomes.

The present results clearly demonstrated that the metabolism of DPT might be CYP-dependent, because the metabolism of DPT to each metabolite was NADPH-dependent (Fig. 2), and because SKF-525A, a well-known CYP inhibitor, significantly inhibited the production of individual DPT metabolites in rat liver microsomes (Table I). In addition, with enriched liver microsomes, four metabolites were identified in the present HPLC condition. As stated in the Results, M3 was only detected in dexamethasone-induced microsomes, indicating that the production of M3 from DPT would be catalyzed by CYP3A as indicated in our recent report (Lee *et al*., 2008). From the production kinetics for each metabolite in Fig. 6, it was hypothesized that M1 and M3 would be formed from M4 as we expected in the recent report (Lee *et al*., 2008). Although the exact structure of M4 was not sure from the LC-ESI/MS whether it is podophyllotoxin or epi-form of podophyllotoxin in our studies, the same MS profiles for M1 and M3 were observed in the present study, when authentic podophyllotoxin was incubated with the rat liver microsomes and β-NADPH (data not shown). Therefore, it will become clear if the configuration of the hydroxyl group on C-7 position of M4 is assigned in the near future.

The isozyme selectivity for DPT metabolism seemed to be quite different from that in human liver microsomes. According to previous reports on the metabolism of DPT by cDNA-expressed human CYP isozymes, DPT would be metabolized by CYP3A4 and CYP2C19, but not by CYP1A2 and CYP2C9 (Vasilev *et al*., 2006; Julsing *et al.,* 2007, Lee *et al*., 2008). Meanwhile, the present results indicated that DPT could be metabolized to M2 and M4 and then metabolite M1 and M3 could be sequentially produced from M4 by CYP 2B and CYP 3A in rat liver microsomes. In addition, CYP 1A and 3A might catalyze the production of M4 in rat liver microsomes. To confirm this possibility, reaction phenotyping is currently under investigation in rat liver microsomes.

Because the present study was carried out in rat liver microsomes, the *in vivo* metabolism of DPT might be required. In this regards, we have recently found an evidence for the Phase II metabolism of DPT in rats. When rats were treated with DPT, at least three different Phase II conjugates with glucuronic acid were detected in urine and/or blood (data not shown). Therefore, the metabolic pathway would be proposed when the Phase II metabolites were fully characterized in the near future.

ACKNOWLEDGEMENTS

This work was supported by a grant from Yeungnam University in 2007.

REFERENCES

Bogucki, D.E. and Charlton, J.L. (1995) An asymmetric synthesis of (-)-deoxypodophyllotoxin. *J. Org. Chem*. **60**, 588-593.

Chen, J.J., Chang, Y.L., Teng, C.M., and Chen, I.S. (2000) Antiplatelet aggregation alkaloids and lignans from *Hernandia nymphaeifolia*. *Planta Med.* **66**, 251-256.

Gordaliza, M., Castro, M.A., Garcia-Gravalos, M.D., Ruiz, P., Miguel del Corral, J.M., and San Feliciano, A. (1994) Antineoplastic and antiviral activities of podophyllotoxin related lignans. *Arch. Pharm.* **327**, 175-179.

Gross, G. (2001) Clinical diagnosis and management of anogenital warts and papillomavirus-associated lesions. *Hautarzt.* **52**, 6-17.

Ikeda, R., Nagao, T., Okabe, H., Nakano, Y., Matsunaga, H., Katano, M., and Mori, M. (1998) Antiproliferative constituents in Umbelliferae plants. IV. Constituents in the fruits of *Anthriscus sylvestris* Hoffm. *Chem. Pharm. Bull.* **46**, 875-878.

Inamori, Y., Kato, Y., Kubo, M., Baba, K., Ishida, T., Nomoto, K., and Kozawa, M. (1985) The biological actions of deoxypodophyllotoxin (anthricin). I. Physiological activities and conformational analysis of deoxypodophyllotoxin. *Chem. Pharm. Bull.* **33**, 704-709.

Jin, M., Moon, T.C., Quan, Z., Lee, E., Kim, Y.K., Yang, J.H., Suh, S.J., Jeong, T.C., Lee, S.H., Kim, C.H., Chang, H.W. (2008) The naturally occurring flavolignan, deoxypodophyllotoxin, inhibits lipopolysaccharide-induced iNOS expression through the NF-kB activation in RAW264.7 macrophage cells. *Biol. Pharm. Bull*. 31, 1312-1315.

Julsing, M.K., Vasilev, N.P., Schneidman-Duhovny, D., Muntendam, R., Woerdenbag, H.J., Quax, W.J., Wolfson, H.J., Ionkova, I., and Kayser, O. (2007) Metabolic stereoselectivity of cytochrome P450 3A4 towards deoxypodophyllotoxin: *In silico* predictions and experimental validation. *Eur. J. Med. Chem.* **19**, 1-9.

Kim, Y., Kim, S.B., You, Y.J., and Ahn, B.Z. (2002) Deoxypodophyllotoxin; the cytotoxic and antiangiogenic component from *Pulsatilla koreana*. *Planta Med.* **68**, 271-274.

Koulman, A., Beekman, A.C., Pras, N., and Quax, W.J. (2003a) The bioconversion process of deoxypodophyllotoxin with *Linum flavum* cell cultures. *Planta Med.* **69**, 739-744.

Koulman, A., Batterman, S., van Putten, F. M. S., Bos, R., and Quax, W. J. (2003b) Lignan profiles of indoor-cultivated *Anthriscus sylvestris. Planta Med.* **69**, 959-961.

Koulman, A., Kubbinga, M.E., Batterman, S., Woerdenbag, H.J., Pras, N., Woolley, J.G., and Quax, W.J. (2003c) A phytochemical study of lignans in whole plants and cell suspension cultures of *Anthriscus sylvestris. Planta Med.* **69**, 733-738.

Lee, S.H., Son, M.J., Ju, H.K., Lin, C.X., Moon, T.C., Choi, H.G., Son, J.K., and Chang, H.W. (2004) Dual inhibition of cyclooxygenase-2 and 5-lipoxygenase by deoxypodophyllotoxin in mouse bone marrow-derived mast cells. *Biol. Pharm. Bull.* **27**, 786-788.

Lee, S.K., Jun, I.H., Yoo, H.H., Kim, J.H., Seo, Y.M., Kang, M.J., Lee, S.H., Jeong, T.C., and Kim, D.H. (2008) Characterization of *in vitro* metabolites of deoxypodophyllotoxin in human and rat liver microsomes using liquid chromatography/tandem mass spectrometry. *Rapid Commun. Mass Spectrom.* **22**, 52-58.

Lim, Y.H., Lee, M.J., Shin, D.H., Chang, H.B., Hong, S.W., Moon, E.Y., Lee, D.K., Yoon, S.J., and Woo, W.S. (1999) Cytotoxic constituents from the roots of *Anthriscus sylvestris*. *Arch. Pharm. Res.* **22**, 208-212.

Lowry, O.H., Rosenbrough, N.J., Farr, A.L., and Randall, R.J. (1951) Protein measurement with the folin phenol reagent. *J. Biol. Chem.* **193**, 265-275.

Masuda, T., Oyama, Y., Yonemori, S., Takeda, Y., Yamazaki, Y., Mizuguchi, S., Nakata, M., Tanaka, T., Chikahisa, L., Inaba, Y., and Okada, Y. (2002) Flow cytometric estimation on cytotoxic activity of leaf extracts from seashore plants in subtropical Japan: Isolation, quantification and cytotoxic action of (-) deoxypodophyllotoxin. *Phytother. Res.* **16**, 353-358.

Molog, G.A., Empt, U., Kuhlmann, S., van Uden, W., Pras, N., Alfermann, A.W., and Petersen, M. (2001) Deoxypodophyllotoxin 6-hydroxylase, a cytochrome P450 monooxygenase from cell cultures of *Linum flavum* involved in the biosynthesis of cytotoxic lignans. *Planta* **214**, 288-294.

Myung, S.W., Kim, H.Y., Min, H.K., Kim, D.H., Kim, M., Cho, H.W., Lee, H.S., Kim, J.K., and Hong, C.I. (2002) The identification of *in vitro* metabolites of CKD-732 by liquid chromatography/tandem mass spectrometry. *Rapid Commun. Mass Spectrom.* **16**, 2048-2053.

Sudo, K., Konno, K., Shigeta, S., and Yokota, T. (1998) Inhibitory effects of podophyllotoxin derivatives on herpes simplex virus replication. *Antivir. Chem. Chemother.* **9**, 263-267.

Vasilev, N.P., Julsing, M.K., Koulman, A., Clarkson, C., Woerdenbag, H.J., Ionkova, I., Bos, R., Jaroszewski, J.W., Kayser, O., and Quax, W.J. (2006) Bioconversion of deoxypodophyllotoxin into epipodophyllotoxin in *E. coli* using human cytochrome P450 3A4. *J. Biotechnol.* **126**, 383-393.

Wong, S.-K., Tsui, S.-K., Kwan, S.-Y., Su, X.-L., and Lin, R.-C. (2000) Identification and characterization of *Podophyllum emodi* by API-LC/MS/MS. *J. Mass Spectrom.* **35**, 1246-1251.